Quantum Electronics **43** (2) 157–161 (2013)

NONLINEAR OPTICAL PHENOMENA

PACS numbers: 42.65.Jx; 42.65.Ky; 52.50.Jm
DOI: 10.1070/QE2013v043n02ABEH015011

Spectrum superbroadening in self-focusing of pulsed vortex beams in air

R.A. Vlasov, V.M. Volkov, D.Yu. Dedkov

Abstract. **Based on numerical simulations, self-focusing of conventional and vortex optical beams produced by femtosecond pulses in air is comparatively analysed. It is shown that, other things being equal, in the case of self-focusing of vortex beams, a significantly higher concentration of energy is observed in the focal spot. As a consequence, there also arises a significant broadening of the space–time spectrum of the focused vortex beam as compared with the vortex-free self-focusing regime. The azimuthal instability of the vortex structure at small initial perturbations of the wave front leads to filamentation of radiation at distances greater than is usually the length of self-focusing.**

Keywords: *femtosecond optical pulses, optical vortices, self-focusing, supercontinuum.*

1. Introduction

Self-focusing of intense femtosecond laser pulses in gaseous and condensed media is accompanied by a radical transformation of the space–time spectrum of radiation, leading to a substantial redistribution of energy in a wide frequency-angular range [1]. The spectrum superbroadening mechanisms, which form the basis of the phenomenon of spatial-temporal phase modulation, include a number of features inherent in femtosecond radiation (slow nonlinear response, nonlinearity dispersion and diffraction dispersion). In addition, depending on the refractive index there is a typical nonlinear component of the plasma arising due to ionisation of the molecules of the medium as a result of multiphoton absorption [2, 3]. Superbroadening of the emission spectrum in self-focusing of intense femtosecond laser pulses in nonlinear media is conventionally called supercontinuum generation – coherent electromagnetic radiation with a continuous spectrum and a high spectral brightness in the visible and near-IR wavelength ranges (see, e.g., reviews [2, 3]). Possibility of producing light pulses with similar characteristics has opened good prospects for laser radiation to be applied in monitoring and remote sensing. To date, the first broadband femtosecond terawatt lidars have already been fabricated. This allows one to gain information about the state of the atmosphere in the wavelength range 400 nm–4 μm, without the need to readjust the carrier frequency of the radiation, which extends the information content of laser sensing [3].

Theoretical and experimental study of the spectral and angular characteristics of radiation and the study of properties of supercontinuum structure formation in self-focusing of high-power pulses in air is described in numerous works [2–12]. The results of research in this area are reflected in a recent review [13]. Among the published studies, to our knowledge, only paper [12] is devoted to the propagation of pulsed beams with a singularity of the wave front (vortex pulses or optical vortices) in the air. The authors of [12] consider the problems of spatial stability of vortex structures, but do not address the issues of spectrum superbroadening. The results of experimental and theoretical investigations of the supercontinuum generation in self-focusing of optical vortices in solids are presented in [14], where the authors observed survival of singular vortex beams upon filamentation, but did not analyse in detail the structural features of the supercontinuum. Meanwhile, as will be shown below, it is the singularity (vortex structure) of the wave front of femtosecond pulses that can drastically and nontrivially change the spectral characteristics and the general picture of self-focusing of such pulses in air.

2. Theoretical model

Propagation of femtosecond optical pulses in air can be described in terms of dimensionless variables $z = Z/D$, $\tau = T/\tau_0$, $r = R/r_0$ and $u = E[P_0/(4\pi r_0^2)]^{1/2}$, based on the following equation (see, e.g., [1–3]):

$$\mathrm{i}\frac{\partial u}{\partial z} + \Delta_\perp u + \varepsilon\frac{\partial^2 u}{\partial \tau^2} - \kappa\frac{\partial^3 u}{\partial \tau^3} - \eta\frac{\partial^2 u}{\partial z\partial \tau} + (\alpha|u|^2 - \delta|u|^4)u$$

$$+ \mathrm{i}\gamma\frac{\partial}{\partial \tau}(|u|^2 u) = \left\{\mu\int_{-\infty}^{\tau}|u|^{2K}d\tau' - \mathrm{i}\nu|u|^{2(K-1)}\right.$$

$$\left. - \frac{\alpha}{\tau_K}\int_{-\infty}^{\tau}\exp\left[-\frac{\tau-\tau'}{\tau_K}\right]|u|^2 d\tau'\right\}u. \qquad (1)$$

The normalised coefficients of equation (1) and the desired function u are expressed via the parameters of the optical pulse and the medium:

$$\alpha = 2k_0 D n_2 \frac{P_0}{4\pi r_0^2}, \quad \gamma = \frac{4k_0 D n_2}{\omega\tau_0}\frac{P_0}{4\pi r_0^2},$$

$$\delta = 2k_0 D n_4\left(\frac{P_0}{4\pi r_0^2}\right)^2, \quad \kappa = \frac{2}{3}D\frac{\partial^3 k}{\partial\omega^3}\tau_0^{-3},$$

R.A. Vlasov B.I. Stepanov Institute of Physics, National Academy of Sciences of Belarus, prosp. Nezavisimosti 68, 220072 Minsk, Belarus; e-mail: r.vlasov@dragon.bas-net.by;
V.M. Volkov, D.Yu. Dedkov Belarusian State University, prosp. Nezavisimosti 4, 220030 Minsk, Belarus; e-mail: volkovvm@bsu.by

Received 27 September 2012; revision received 21 November 2012
Kvantovaya Elektronika **43** (2) 157–161 (2013)
Translated by I.A. Ulitkin

$$\nu = 2D\beta_K\left(\frac{P_0}{4\pi r_0^2}\right)^{K-1}, \quad \mu = \frac{2k_0 D\sigma_K\rho_{\rm nt}\tau_0}{\rho_{\rm c}}\left(\frac{P_0}{4\pi r_0^2}\right)^K,$$

$$\varepsilon = 2D\frac{\partial^2 k}{\partial\omega^2}\tau_0^{-2}, \quad \eta = \tau_0^{-1}\omega_0^{-1}.$$

Here P_0 is the critical self-focusing power; $k = 2\pi/\lambda$; $k_0 = 2\pi/\lambda_0$; λ_0 is the wavelength; $D = \pi r_0^2/\lambda_0$ is the diffraction length; β_K and σ_K are the photon absorption and multiphoton ionisation coefficients; $\rho_{\rm nt}$ and $\rho_{\rm c}$ are the effective density of neutral molecules and the critical plasma density; and $K = 8$ is the integer constant characterising the multiplicity of the number of photons in the effects of multiphoton absorption by oxygen molecules (ionisation threshold of nitrogen is higher than that of oxygen; therefore, only the ionisation of oxygen molecules is considered). The parameter τ_K is defined as the ratio of the relaxation time of the cubic nonlinearity to the pulse duration. The constants ε and κ characterise the group velocity dispersion of momentum in the second and third approximations of the dispersion theory, γ describes the dispersion of nonlinearity, and α and δ take into account the instantaneous and inertial corrections to the nonlinear dependence of the refractive index on the radiation intensity. The terms of the equation with the coefficients μ and ν take into account the effects of nonlinear self-action caused by ionisation of the medium under the influence of multiphoton absorption and tunnelling, and the term with coefficient η describes the dispersion diffraction. When pulsed radiation (wavelength, 800; duration, τ_0 = 100 fs; and initial beam radius, r_0 = 3 mm) propagates in air, the coefficients in equation (1) have the following values: $\alpha = 0.52$, $\gamma = 4.3\times10^{-3}$, $\eta = 4.2\times10^{-3}$, $\delta = 1.5\times10^{-5}$, $\varepsilon = -0.14$, $\kappa = 1.6\times10^{-4}$, $\mu = 3.8\times10^{-31}$, $\nu = 7.4\times10^{-29}$, $\tau_K = 0.7$.

The mechanism of impact ionisation in this case can be ignored, because the pulse duration is much smaller the electron–atom collisions.

Most coefficients of the studied equation make sense of small parameters for the initial radiation parameters. Because of this, the effects associated with the relevant terms of the equation make a negligible contribution to the dynamics of the pulsed beam at the initial stage of its evolution. Under the influence of the nonlinear self-focusing of the pulsed beam, its spatial-temporal scales vary considerably, which is reflected in a significant broadening of the space–time spectrum of radiation and the appearance of local features of the field intensity at which each of the terms in equation (1) makes a commensurable contribution to the overall picture of the phenomena associated with self-focusing of radiation in air.

To describe the transverse field structure, use is made of the polar coordinates r and φ [$\Delta_\perp = r^{-1}\partial_r(r\partial_r) + r^{-2}\partial_\varphi^2$]. The initial conditions for (1) are given as

$$u(r,\varphi,\tau,z=0) = u_0(r/r_0)^m \exp[-(r/r_0)^2 - \tau^2 + im\varphi], \qquad (2)$$

where $m = 0, \pm1, \pm2$ is the topological charge of the pulsed beam [12, 13, 15].

3. Results of the numerical analysis

Within the framework of the developed mathematical model (1), (2), we studied numerically the dynamics of conventional and vortex pulsed optical beams in air. For the numerical analysis of the problem use was made of the fractional-step spectral-difference method, the details of which are described elsewhere. Application of the Fourier method to the variables τ and φ with the difference approximation on an irregular grid over r provided sufficient computational accuracy for a relatively small size of the computational grid. The number of grid nodes in time $N_\tau = 10^{12}$ ensured in the focal spot the spectral resolution at wavelengths from the near-UV to the radio band. The nonuniform grid in the radial direction at a number of nodes $N_r = 256$ allowed one to obtain in the focal spot the spatial resolution with a step of $h = (0.6 - 10.0)\times10^{-6}$ m. The analysis of the three-dimensional problem showed that in the azimuthal direction it is sufficient to use a grid with the number of nodes $N_\varphi = 32$. The step on the evolutionary variable z was chosen in the range of $10^{-4} - 10^{-7}$, depending on the maximum radiation intensity and in such a way that the maximum phase increment due to the nonlinear phase modulation of the complex envelope of the solution at each step did not exceed 0.02–0.05 rad.

We investigated the properties of emission spectrum superbroadening in self-focusing and analysed the major differences in the behaviour of conventional and vortex pulsed beams in terms of the structure of the spectral supercontinuum.

For comparison, we considered self-focusing of conventional and vortex pulsed beams with topological charges $m = 0$ and 1, respectively, under conditions of the same power (energy) and pulse duration of 100 fs (half-width of the field amplitude level $u_{\max}/e$). To provide approximately the same self-focusing length of the conventional and vortex beams we assumed that the pulsed beam radius was $r_0 = 6$ mm at $m = 0$ and 3 mm at $m = 1$. The peak power was set equal to the twentyfold excess of the critical power necessary for self-focusing of a stationary beam for the given parameters of the medium nonlinearity. It should be noted that the critical power necessary for self-focusing of the vortex beam with a unit topological charge is more than three times the usual critical self-focusing power of the conventional beam [14]; therefore, in the numerical experiments, the multiplicity of the excess of the critical power of the vortex beam was lower than that of the conventional beam.

Consider the features of self-focusing of conventional pulsed beams with a Gaussian spatial and temporal profile. Because of the nonlinearity inertia, leading self-focusing is observed not in the cross section corresponding to the maximum pulse power, but with some delay (Fig. 1, $z = 0.128$). Further dynamics is characterised by the movement of the focus in the direction of the leading edge, and already at $z = 0.130$ its position is ahead (in time) of the position of the cross section corresponding to the maximum power, while behind the focus divergent radiation, experiencing self-focusing, is observed. Thus, the nonlinearity inertia leads to the characteristic nonstationary self-focusing, which is at an early stage manifests itself in the movement of the primary focus at a velocity that is higher than the group velocity of the propagating pulse.

The subsequent propagation of the pulsed beam is characterised by an increasing amplitude modulation of radiation both in the longitudinal and transverse cross sections, which is also reflected in the broadening of the space–time spectrum. The beam radius in the case of self-focusing is reduced by approximately two orders of magnitude, and approximately the same spatial scale is typical of the pulse intensity modulation in time (Fig. 1).

Self-focusing of the vortex beam is characterised primarily by an increase in the self-focusing length. This is a consequence of a lower multiplicity of the excess over the critical

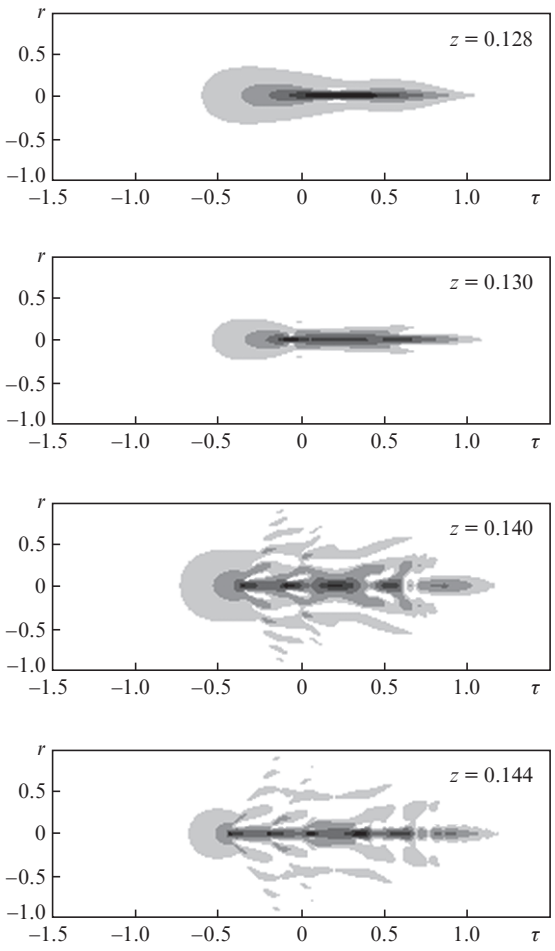

Figure 1. Spatiotemporal distributions of the field amplitude of the pulsed beam with the initial Gaussian spatial and temporal profile at $m = 0$ in the process of self-focusing.

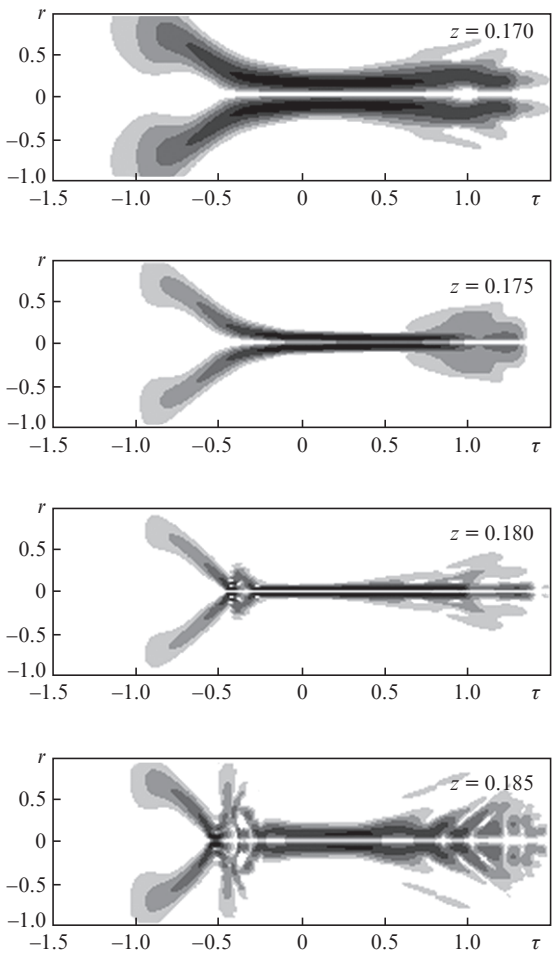

Figure 2. Spatiotemporal distributions of the field amplitude of a pulse vortex beam with a topological charge $m = 1$ in the process of self-focusing.

power of the vortex beam. Nonstationary self-focusing of the vortex beams manifests itself in the formation of a horn-shaped structure of their spatial and temporal profile. In this case, the leading self-focusing of the trailing edge of the pulse is clearly traced on the spatial and temporal profile of the pulse (Fig. 2, $z = 0.170$ and 0175).

Among the differences observed during the self-focusing of vortex pulses as compared to conventional pulses, we note a significant decrease in the intensity modulation of the radiation in the longitudinal and transverse cross sections. Reducing spatial aberrations of vortex pulses is, apparently, due to an increase in the energy threshold of self-focusing, since it is the multiplicity of the excess over the critical power that characterises the distortion of the original space–time structure. In the focal region, the critical power is usually localised, while the periphery of the beam is focused with delay, interfering with a divergent radiation, which has already experienced this self-focusing. Such interference is manifested in concentric rings in the transverse intensity distribution, formed behind the focus of a nonlinear beam having a power that is significantly higher than the critical one [4].

It is notable that the peak intensity during the self-focusing of the pulsed vortex beam significantly exceeds a similar value for conventional pulses (Fig. 3). Taking into account the fact that the radiation power in the focal spot of the vortex beam is many times higher than the power of the focused conventional beam, one should expect more significant manifestations of plasma nonlinearity due to multiphoton absorption and ionisation of air. When the intensity of radiation is less than a certain threshold, the pulse energy remains unchanged.

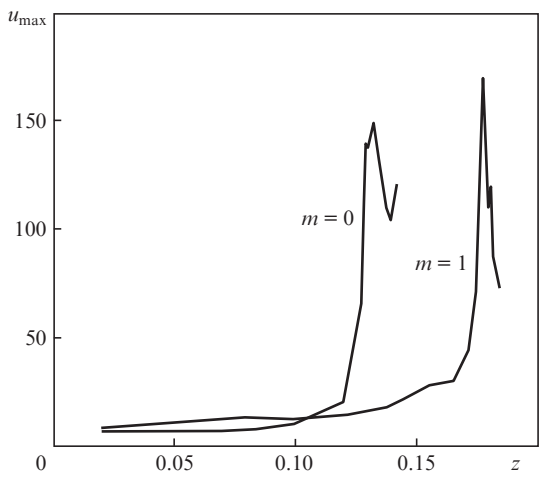

Figure 3. Peak field amplitude dynamics $u_{max} = \max_{r,\tau}[|u(r,\tau,z)|]$ of pulsed conventional ($m = 0$) and vortex ($m = 1$) beams during the self-focusing in air.

The excess over the ionisation threshold during the self-focusing leads to dissipative processes that result in energy loss. The energy loss in self-focusing a vortex pulse is over 3% of the initial value, which is more than an order of magnitude higher than a similar loss in self-focusing a conventional pulse; the loss in this case does not exceed tens of percent. The peak intensity during the self-focusing is largely determined not only by the plasma nonlinearity, but also by defocusing correction of the fifth degree. If we neglect the latter, that is, in the case of $\delta = 0$, the energy loss of the conventional pulse becomes greater than 1% and in the case of the vortex pulse the energy loss is close to 20%.

The picture of self-focusing is formed under the influence of the nonlinear phase modulation of the pulse. The superbroadening of the spectrum during the self-focusing is achieved by the simultaneous influence of the cubic and plasma nonlinearities. The substantial inertia of the plasma nonlinearity (its relaxation time exceeds manifold the pulse duration) leads to the fact that at the leading edge of the primary focus the phase modulation due to the cubic nonlinearity dominates, while at the trailing edge an important role is played by the plasma nonlinearity that is opposite in sign. This mechanism of phase modulation under the influence of competing nonlinearities of opposite sign makes a major contribution to the formation of the space–time structure and spectral characteristics of radiation when high-power pulsed laser beams propagate in the air.

Figure 4 shows the spectral and angular characteristics of the conventional and vortex pulsed beams during the self-focusing. As above, we consider the case of the 100-fs pulsed beams with a peak power which is about twenty times higher than the critical self-focusing power. The scattering angle of the spectral components of the pulse is calculated in the standard way: $\tan\theta = k_\perp/k_\parallel$, where $k_\parallel$ and $k_\perp$ are the longitudinal and transverse components of the wave vector. The frequency-angular spectrum was calculated using the Fourier transform of the complex envelope of the pulse. The spectral characteristics of optical pulses during the self-focusing in gases and liquids are investigated theoretically and experimentally in [4, 6, 8] (see also reviews [2, 3, 13]). The results of numerical simulations presented in Figs 1 and 4 are in qualitative agreement with the presently known results [3, 4, 13]. The power and peak intensity localised in the focus of the vortex beam exceed the same parameters during the self-focusing of conventional pulses with the same initial energy and duration. As a consequence, the characteristic broadening of the space–time spectrum during the self-focusing of the vortex beam is much larger than in the vortex-free regime. The width of the angular spectrum, as shown in Fig. 4, during the self-focusing of the vortex beam is about ±0.25°, while for conventional beams with the same energy, it is within ±0.1° [4]. Qualitatively, the spectrum of the focused vortex pulses is characterised by the conical emission dominating in the long-wavelength wing, whereas in the spectrum of conventional beams conical emission dominates in the short-wavelength region [2, 4, 6, 8].

Another significant difference of the propagation dynamics of pulsed optical vortex beams is their inherent azimuthal instability that leads to the destruction of the vortex structure and filamentation of radiation into several channels diverging from the axis of the initial beam [12, 15]. In contrast to the media with anomalous dispersion, where there are stable propagation regimes of vortex pulsed beams with a single topological charge [16], in media with cubic saturable nonlinearity (such as air), one can observe an absolute instability of the vortex structure of pulses [12]. However, the theoretical estimates indicate the possibility of a stable propagation of vortex pulsed beams at a distance of several hundred meters [12]. Numerical experiments have shown that at small initial perturbations of the vortex mode, vortex pulse filamentation is generally observed at distances greater than the length of the nonlinear self-focusing.

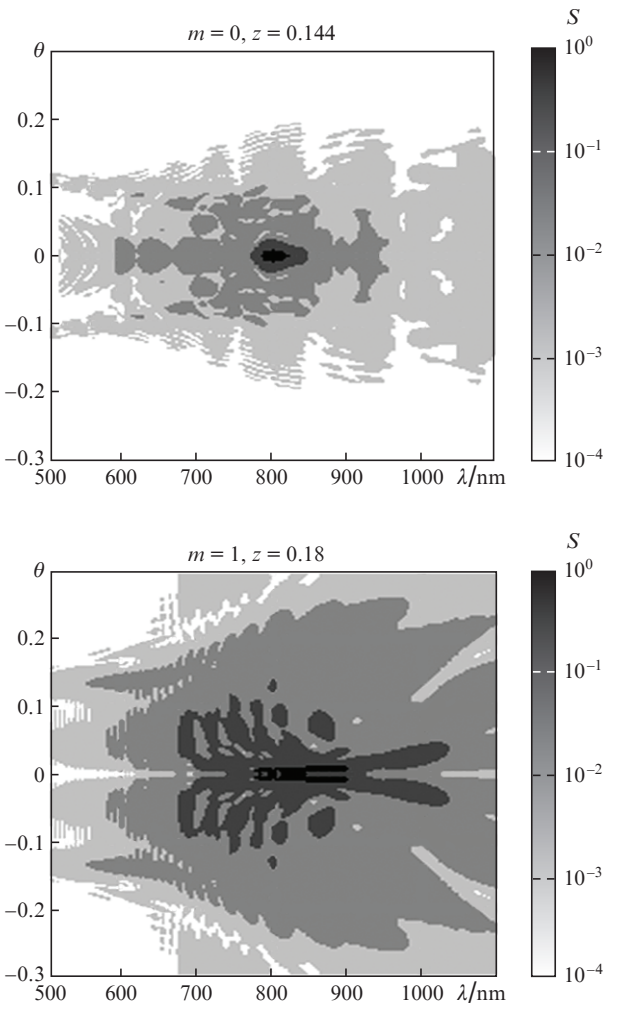

Figure 4. Frequency-angular distributions of the relative spectral densities S of the conventional and vortex pulsed beams which have experienced self-focusing.

Figure 5 shows the propagation dynamics of a pulsed vortex beam, which has already experienced the self-focusing. The initial parameters of the pulse are the same as in the above case (see Figs 2 and 3). The iso-surfaces of the vortex pulse intensity are coloured in accordance with the values of the phase of the complex envelope of the field, which allows one, along with the development of amplitude modulation to observe simultaneously the development of the spatial-temporal phase modulation. The data presented demonstrate the nonstationary self-focusing, which leads to the formation of the characteristic horn-shaped structure in the intensity distribution at the leading edge of the pulse. Growth of azimuthal perturbations leading to the transverse instability of the ring structure of the optical vortex dominates at the trailing edge of the pulse.

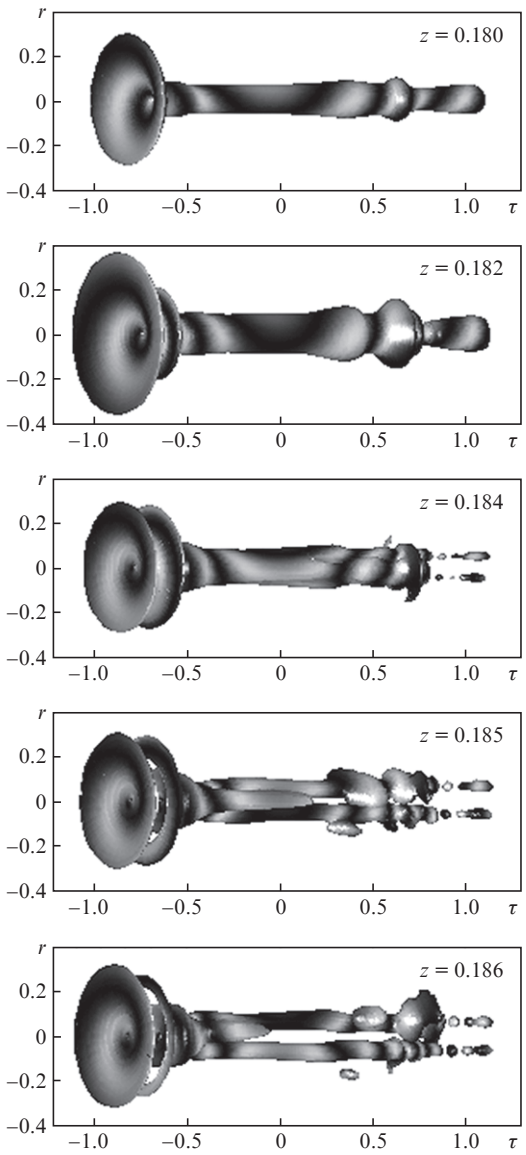

Figure 5. Destruction of the pulsed vortex optical beam during the self-focusing in air. The brightness of colour of intensity iso-surfaces, corresponding to the phase of the complex field envelope, allows one to see the vortex structure and the growing phase modulation of the pulse.

4. Conclusions

The presented results of the comparative numerical analysis of the propagation dynamics of conventional and vortex pulses in air have revealed some significant differences inherent in the self-focusing of the latter. The frequency and angular spectra are significantly broadened during the self-focusing of vortex beams in comparison with the vortex-free regimes. This difference is due to the higher peak intensity and localisation of the vortex pulse of a higher power in the focal spot. The azimuthal instability of vortex pulsed beams in media with normal dispersion limits the distance of their stable propagation in air. However, at sufficiently small initial amplitude and phase perturbations of the wave front of the initial pulse the distance of stable propagation of optical vortices with topological charge $m = 1$ can exceed the length of the nonlinear self-focusing. The differences demonstrated point to the fact that the use of the vortex pulses in the problems of remote sensing of the atmosphere is quite promising.

References

1. Akhmanov S.A., Vysloukh V.A., Chirkin A.S. *Optics of Femtosecond Laser Pulses* (New York: AIP Press, 1992; Moscow: Nauka, 1988).
2. Chin S.L., Hosseini S.A., Liu W., Luo Q., Theberge F., Aközbek N., Becker A., Kandidov V.P., Kosareva O.G., Schroeder H. *Can. J. Phys.*, **83**, 863 (2005).
3. Berge L., Skupin S., Nuter R., Kasparian J., Wolf J.-P. *Rep. Prog. Phys.*, **70**, 1633 (2007).
4. Kandidov V.P., Kosareva O.G., Koltun A.A. *Kvantovaya Elektron.*, **33**, 69 (2003) [*Quantum Electron.*, **33**, 69 (2003)].
5. Ando T., Fujimoto M. *Phys. Rev. E.*, **72**, 026706 (2005).
6. Golubtsov I.S., Kosareva O.G. *Opt. Zh.*, **69**, 21 (2002).
7. Kandidov V.P., Shlenov S.A., Kosareva O.G. *Kvantovaya Elektron.*, **39**, 205 (2009) [*Quantum Electron.*, **39**, 205 (2009)].
8. Trushin S.A., Panja S., Kosma K., Schmid W.E., Fuss W. *Appl. Phys. B*, **80**, 399 (2005).
9. Geints Yu.E., Zemlyanov A.A. *Kvantovaya Elektron.*, **40**, 121 (2010) [*Quantum Electron.*, **40**, 121 (2010)].
10. Balashov A.D., Pergament A.Kh. *Kvantovaya Elektron.*, **36**, 825 (2006) [*Quantum Electron.*, 36, 825 (2006)].
11. Geints Y.E., Zemlyanov A.A., Kabanov A.M., Bykova E.E., Apeksimov D.V., Bukin O.A., Sokolova E.B., Golik S.S., Ilyin A.A. *Appl. Opt.*, **50**, 5291 (2011).
12. Vinçotte A., Berge L. *Phys. Rev. Lett.*, **95**, 193901 (2005).
13. Wang T.J., Marceau C., Wu J., Liu J.S., Kosareva O., Panov N., Chen Y.P., Daigle J.F., Yuan S., Azarm A., Liu W.W., Seideman T., Zeng H.P., Richardson M., Li R., Xu Z.Z. *Laser Phys.*, **22**, 1 (2012).
14. Neshev D.N., Dreischuh A., Maleshkov G., Samoc M., Kivshar Yu.S. *Opt. Express*, **18**, 18368 (2010); Maleshkov G., Neshev D.N., Petrova E., Dreischuh A. *J. Opt.*, **13**, 064015 (2011).
15. Kruglov V.I., Logvin Yu.A., Volkov V.M. *J. Mod. Opt.*, **39**, 2277 (1992).
16. Kivshar Yu.S., Agrawal G.P. *Optical Solitons. From Fiber to Photonic Crystal* (New York: Academic Press, 2003).